APPLIED AND ENVIRONMENTAL MICROBIOLOGY, Jan. 2006, p. 901–907 Vol. 72, No. 1
0099-2240/06/$08.00+0 doi:10.1128/AEM.72.1.901–907.2006

Role of Tryptophan Residues in Toxicity of Cry1Ab Toxin from *Bacillus thuringiensis*

Cristopher Padilla,[1] Liliana Pardo-López,[1] Gustavo de la Riva,[1] Isabel Gómez,[1] Jorge Sánchez,[1] Georgina Hernandez,[1] Maria Eugenia Nuñez,[2] Marianne P. Carey,[3] Donald H. Dean,[4] Oscar Alzate,[5] Mario Soberón,[1] and Alejandra Bravo[1]*

Departamento de Microbiología Molecular, Instituto de Biotecnología Universidad Nacional Autónoma de México, UNAM, Apdo. Postal 510-3, Cuernavaca, 27510 Morelos, Mexico[1]; Centro de Desarrollo e Investigación Agropecuaria UAEM, Av. Universidad 1001, Cuernavaca, 62210 Morelos, Mexico[2]; Department of Biochemistry, Case Western Reserve University, Cleveland, Ohio 44106[3]; Department of Biochemistry, Ohio State University, Columbus, Ohio 43210[4]; and Department of Neurobiology, Duke University Medical Center, Durham, North Carolina 27710[5]

Received 2 August 2005/Accepted 29 October 2005

Bacillus thuringiensis **produces insecticidal proteins (Cry protoxins) during the sporulation phase as parasporal crystals. During intoxication, the Cry protoxins must change from insoluble crystals into membrane-inserted toxins which form ionic pores. The structural changes of Cry toxins during oligomerization and insertion into the membrane are still unknown. The Cry1Ab toxin has nine tryptophan residues; seven are located in domain I, the pore-forming domain, and two are located in domain II, which is involved in receptor recognition. Eight Trp residues are highly conserved within the whole family of three-domain Cry proteins, suggesting an essential role for these residues in the structural folding and function of the toxin. In this work, we analyzed the role of Trp residues in the structure and function of Cry1Ab toxin. We replaced the Trp residues with phenylalanine or cysteine using site-directed mutagenesis. Our results show that W65 and W316 are important for insecticidal activity of the toxin since their replacement by Phe reduced the toxicity against *Manduca sexta*. The presence of hydrophobic residue is important at positions 117, 219, 226, and 455 since replacement by Cys affected either the crystal formation or the insecticidal activity of the toxin in contrast to replacement by Phe in these positions. Additionally, some mutants in positions 219, 316, and 455 were also affected in binding to brush border membrane vesicles (BBMV). This is the first report that studies the role of Trp residues in the activity of Cry toxins.**

Among the biopesticides, *Bacillus thuringiensis* is a viable alternative for the control of insects in agriculture and as disease vectors, which is important to public health. *B. thuringiensis* produces insecticidal proteins (Cry protoxins) during the sporulation phase as parasporal crystals. Cry toxins are highly specific to their target insect, safe for humans, vertebrates, and plants, and biodegradable (26). The parasporal crystals are ingested by a susceptible insect and solubilized in the midgut lumen. Proteinase enzymes present in the insect gut lumen activate the solubilized Cry protoxins. The activated toxin binds to receptors located in the apical brush border microvillus membrane (5). Two groups of different Cry1As toxin receptors, cadherin-like proteins (BT-R_1 and BT-R_{175}) (18, 28) and aminopeptidase N (11, 24), have been described previously. Recent data demonstrated that Cry toxin binding to BT-R_1 induces a conformational change that results in the cleavage of helix α-1 and the formation of a prepore oligomeric structure composed of probably four monomers (8, 23). A tetrameric toxin structure was observed by atomic force microscopy of Cry1A toxin inserted in artificial monolayers (29). We showed that, after the interaction of Cry1Ab with BT-R_1, the prepore structure binds aminopeptidase N, and this complex is driven into detergent-resistant membranes or lipid rafts, where the prepore is inserted into the membrane, leading finally to ion leakage, cell lysis, and insect death (5).

The solution of the three-dimensional structure of Cry toxins (Cry3A, Cry1Aa, and Cry2Aa) was an important advance in the understanding of the mode of action of these toxins (9, 14, 17). The structural changes of Cry toxins during oligomerization and insertion into the membrane are still not fully understood.

Upon oligomerization, Cry1Ab toxin undergoes a conformational change which leads to rearrangement of Trp side chains, reducing the accessibility of soluble quenchers to Trp residues (23). Upon membrane penetration, a second change in conformation occurs favoring the possibility that Trp residues come in close contact with the membrane and possibly anchor the prepore to the lipid bilayer (23). Cry1Ab toxin has nine Trp residues, seven are located in domain I, the pore-forming domain, and two are located in domain II, which is involved in receptor recognition (9). Eight Trp residues are highly conserved within the whole family of three-domain Cry proteins (4), suggesting an essential role for these residues in the structural folding and function of the toxin. Only the Cry1A toxins have an extra Trp residue (W219), located in the loop between helices α-6 and α-7, that is highly exposed to the solvent (9). Trp 210 is also highly exposed to the solvent, followed by Trp 73 and Trp 117. The rest of the Trp residues (W65, W182, W226, W316, and W455) are buried within the toxin structure (9).

In this work, the Trp residues of Cry1Ab toxin were replaced by phenylalanine or cysteine by site-directed mutagenesis and

* Corresponding author. Mailing address: Departamento de Microbiología Molecular, Instituto de Biotecnología UNAM, Apdo. Postal 510-3, Cuernavaca, 27510 Morelos, Mexico. Phone: (52) 7773 291635. Fax: (52) 7773 172388. E-mail: bravo@ibt.unam.mx.

TABLE 1. Mutagenic primers used in this work

Primer	Size	Sequence (5′ to 3′)[a]	5′ Position
W65Fdir	30-mer	GTTGATATAATA**TTT**GGAATTTTTGGTCCC	180
W65Frev	30-mer	GGGACCAAAAATTCC**AAA**TATTATACAAC	210
W73Fdir	34-mer	GGAATTTTTGGTCCCTCTCAA**TTT**GACGCATTTC	195
W73Frev	34-mer	GAAATGCGTC**AAA**TTGAGAGGGACCAAAAATTCC	229
W117Fdir	41-mer	CGCAGAATCTTTTAGAGAG**TTT**GAAGCAGATCCTACTAATC	329
W182Fdir	35-mer	GTGTTTGGAACAAAGG**TTT**GGATTTGATGCCGCGAC	528
W182Frev	35-mer	GTCGCGGCATCAAATCC**AAA**CCTTTGTCCAAACAC	563
W210Fdir	40-mer	CAACTATACAGATCATGCTGTACGC**TTT**ACAATACGGGA	603
W210Frev	40-mer	TCCCGTATTGTA**AAA**GCGTACAGCATGATCTGTATAGTTG	643
W219Frev	41-mer	CTTATCCAATCTCTAGAATCCGGTCC**AAA**TACTCGCTCTAA	683
W219Fdir	41-mer	TTAGAGCGTGTA**TTT**GGACCGGATTCTAGAGATTGGATAAG	642
W226Fdir	47-mer	GTATGGGGACCGGATTCTAGAGAT**TTT**ATAAGATATAATCAATTTAG	652
W226Frev	47-mer	CTAAATTGATTATATCTTAT**AAA**ATCTCTAGAATCCGGTCCCCATAC	699
W316Fdir	41-mer	CGGATGCTCATAGAGGAGAATATTAT**TTT**CAGGGCATCAA	919
W316Frev	41-mer	TTGATGCCCTGA**AAA**ATAATATTCTCCTCTATGAGCATCCG	960
W455Fdir	43-mer	AGAGCTCCTATGTTCTCT**TTT**ATACATCGTAGTGCTGAATTTA	1345
W455Frev	43-mer	TAAATTCAGCACTACGATGTAT**AAA**AGAGAACATAGGAGCTCT	1388
W455Crev	32-mer	GCACTACGATGTAT**ACA**AGAGAACATAGGAGC	1380
W455Cdir	32-mer	GCTCCTATGTTCTCT**TGT**ATACATCGTAGTGC	1348
W117Crev	42-mer	GGATTAGTAGGATCTGCTTC**ACA**CTCTCTAAAAGATTCTGCG	371
W117Cdir	42-mer	CGCAGAATCTTTTAGAGAG**TCT**GAAGCAGATCCTACTAATCC	329
W65Cdir	25-mer	GATATAATA**TGT**GGAATTTTTGGTC	184
W73Cdir	28-mer	CCCTCTCAA**TGT**GACGCATTTCTTGTAC	208
W117Cdir	26-mer	TTTAGAGAG**TGT**GAAGCAGATCCTAC	339
W182Cdir	22-mer	AAAGG**TGT**GGATTTGATGCCGC	538
W210Cdir	25-mer	GTACGC**TGT**TACAATACGGGATTAG	622
W219Crev	27-mer	ATCCGGTCC**ACA**TACACGCTCTAATCC	666
W226Crev	27-mer	ATATCTTAC**ACA**ATCTCTAGAATCCGG	687
W316Crev	25-mer	GATGCCCTGA**ACA**ATAATATTCTCC	959

[a] Mutagenic codons are in boldface.

the role of each tryptophan residue in the structure and function of this toxin was analyzed.

MATERIALS AND METHODS

Construction of tryptophan mutants. Phenylalanine mutagenesis of Trp residues of the *cry1Ab* gene was based on the QuikChange site-directed mutagenesis kit (Stratagene, La Jolla, CA). The recombinant pHT315 plasmid (13) harboring the wild-type *cry1Ab* gene (pHT315-1Ab) was used as the template for single substitutions of W455F and W455C. For substitutions of other Trp residues, the DNA template was a 1,177-bp ClaI fragment of *cry1Ab* cloned into pBluescript-SK (Stratagene, La Jolla, CA). The cysteine mutagenesis of Trp residues was also performed with the ClaI fragment of *cry1Ab* cloned into pBluescript-SK by the overlap-extension PCR method of site-directed mutagenesis as previously described (16). Table 1 shows the mutagenic primers used in this work. The recombinant plasmids obtained for each mutant were verified by automated DNA sequencing at Instituto de Biotecnologia, UNAM facilities. Mutant ClaI fragments were restricted and subcloned in pHT315-1AbΔClaI. Acrystalliferous *B. thuringiensis* strain 407, kindly provided by Didier Lereclus, Institute Pasteur, Paris, France, was transformed with the mutated *cry1Ab* genes and selected in Luria broth at 30°C supplemented with 10 μg ml^{-1} erythromycin (13).

Cry1Ab purification. Crystals of wild-type or mutant Cry1Ab proteins were produced in the *B. thuringiensis* transformant strains grown for 3 days at 29°C in nutrient broth sporulation medium (12) supplemented with 10 μg ml^{-1} erythromycin. After complete sporulation, crystals were observed under phase-contrast microscopy and then purified by sucrose gradients as reported previously (27) and solubilized in extraction buffer (50 mM Na_2CO_3, pH 10.5, 0.2% β-mercaptoethanol). The monomeric structure of the toxin was produced by activation of protoxin with trypsin in a mass ratio of 1:20 for 1 h at 37°C. Phenylmethylsulfonyl fluoride (PMSF) was added to a final 1 mM concentration to stop proteolysis. The oligomeric structure of the toxin was produced by incubation of protoxin for 1 h with scFv73 antibody in a mass ratio of 1:4 and digestion with 5% midgut juice from *Manduca sexta* larvae for 1 h at 37°C as described previously (8, 23). PMSF was added in a final 1 mM concentration to stop proteolysis.

Purification of scFv73 antibody. scFv73 antibody was purified from *Escherichia coli* cells by a Ni-agarose column as described previously (8).

Bioassays. Toxicity of wild-type Cry1Ab toxin and the Trp mutants was assayed in first instar *M. sexta* larvae. A total of 24 larvae in 24-well plaques (Cell Wells; Corning Glass Works, Corning, New York) were fed different doses (from 1 to 2,000 ng cm^{-2}) of toxin in an artificial diet (Bio-Serv). Bioassays were performed at 28°C with 65% ± 5% relative humidity and a light-dark photoperiod of 16:8 h. Mortality was recorded after 7 days, and the 50% lethal concentration (LC_{50}) was analyzed with Probit software.

Binding assay. Binding analysis and homologous competition of wild-type and mutant toxins to *M. sexta* BBMV were performed in a binding assay as previously described (3). Trypsin-activated Cry1Ab wild-type toxin was biotinylated by using biotinyl-*N*-hydroxysuccinimide ester (RPN28; Amersham) according to the manufacturer's indications. Binding was performed in 100 μl of binding buffer (phosphate-buffered saline, 0.1% wt/vol bovine serum albumin, 0.1% vol/vol Tween 20, pH 7.6). Biotinylation of Cry1Ab toxin does not affect the biological activity since toxicity of biotinylated toxin is similar to that of the unlabeled toxin (data not shown). Ten μg BBMV proteins were incubated with 10 nM biotinylated toxin in the presence (or absence) of a 50- to 1,000-fold excess of unlabeled Cry1Ab toxin for 1 h. The unbound toxin was removed by centrifugation for 10 min at 14,000 × *g*. The BBMV were suspended in 100 μl of binding buffer and washed twice with the same buffer. Finally, the BBMV were suspended in 20 μl of phosphate-buffered saline, pH 7.6, and an equal volume of Laemmli sample loading buffer 2× (0.125 M Tris-HCl, pH 6.8, 4% sodium dodecyl sulfate [SDS], 20% glycerol, 10% 2-mercaptoethanol, 0.01% bromophenol blue) was added. Samples were boiled for 5 min, loaded in SDS-polyacrylamide gel electrophoresis (PAGE) gels, and electrotransferred to nitrocellulose membranes. The biotinylated protein that remained bound to the vesicles was visualized by incubating with streptavidin-peroxidase conjugate (1:4,000 dilution) for 1 h, followed by luminol (ECL, catalog no. RPN 2109; Amersham) as indicated by the manufacturer.

Western blotting. Cry1Ab wild-type or Trp mutant toxins were separated in SDS-PAGE and transferred onto a nitrocellulose membrane. Proteins were detected with polyclonal anti-Cry1Ab (1/10,000; 1 h) and a goat anti-rabbit antibody coupled with horseradish peroxidase (Sigma, St. Louis, MO) (1/5,000; 1 h), followed by SuperSignal chemiluminescence substrate (Pierce, Rockford, IL) as indicated by the manufacturer.

BBMV. BBMV from 5th-instar *M. sexta* larvae were prepared and analyzed as previously reported (30). The vesicles were dialyzed overnight against 400 vol-

TABLE 2. Toxicity of wild-type and Trp mutants of Cry1Ab toxin against *M. sexta* larvae

δ-Endotoxin	Crystal[a]	LC_{50} ng/cm^2 (95% fiducial limits)	δ-Endotoxin	Crystal[a]	LC_{50} ng/cm^2 (95% fiducial limits)
Wt Cry1Ab	Bip	2.3 (1.2–3.5)			
W65F	Bip	11.47 (3.5–26.8)	W65C	NCI	
W73F	Bip	0.7 (0.2–1.6)	W73C	Bip	3.1 (1.6–5.6)
W117F	Bip	4.9 (3.5–6.6)	W117C	NCI	
W182F	Bip	3.1 (1.6–5.0)	W182C	Bip	4.0 (2.3–6.2)
W210F	Bip	1.5 (0.9–2.5)	W210C	Bip	4.2 (1.9–7.3)
W219F	Bip	1.0 (0.2–1.8)	W219C	Bip	17.8 (10.8–27.2)
W226F	Bip	2.5 (2.1–3.2)	W226C	NCI	
W316F	Bip	35.4 (22.7–52.5)	W316C	Small Bip	82.7 (34.5–235)
W455F	Bip	1.6 (0.5–2.8)	W455C	Small Bip	17.6 (7.5–35.1)

[a] Crystal formation was observed under phase-contrast microscopy. Bip, bipiramidal; NCI, no crystal inclusion observed.

umes of 150 mM KCl, 10 mM HEPES-HCl (pH 7.5) (Sigma, St. Louis, MO) and sonicated (Branson 1200 sonic bath; Branson, Danbury, CT) for six periods of 30 s each at 25°C in the same solution.

Pore formation activity. Membrane potential was monitored with the positively charged fluorescent dye 3,3′-dipropylthiodicarbocyanine [Dis-C_3-(5); Molecular Probes] as previously described (15). Fluorescence (F) was recorded at 620/670 nm excitation/emission wavelengths in an Aminco SLM spectrofluorometer. Hyperpolarization causes dye internalization in the BBMV and a decrease in fluorescence, while depolarization causes the opposite effects. BBMV (10 μg) previously loaded with 150 mM KCl were suspended in 900 μl of the following buffer system: 150 mM CsCl, 1 mM $CaCl_2$, and 10 mM HEPES-HCl, pH 7. After equilibration of the dye, 3 nM Cry1Ab oligomeric prepore toxin was added. Changes in membrane potential were monitored by successive additions of KCl (4, 8, 12, 16, 32, and 64 mM, final concentrations) to the BBMV suspension. Numbers (1 to 6) above the traces correspond to each one of the KCl additions. The same amount of the toxin buffer was added for control traces. Analyses of the slope (m) of ΔF (%) versus K^+ equilibrium potential (E_K) (millivolts) are reported in this work. E_K was calculated with the Nernst equation. Membrane potential determinations were performed four times.

Protein concentration. Protein concentration was determined by the Bradford assay using bovine serum albumin as standard and by absorbance at 280 nm using the extinction coefficient $E_m^{280} = 5{,}700\ M^{-1}/cm^{-1}$ for Cry1Ab toxin.

RESULTS

Isolation of Cry1Ab mutant toxins. Each one of the nine tryptophan residues of the wild-type Cry1Ab toxin was substituted by phenylalanine or cysteine by using site-directed mutagenesis. *B. thuringiensis* cells transformed with mutated genes were grown in sporulation medium, and crystals were observed under phase-contrast microscopy and purified by sucrose gradient centrifugation. Mutants W65C, W117C, and W226C did not produce crystal inclusion bodies, while mutants W316C and W455C produced very small bipyramidal crystals (Table 2). The rest of the Trp substitutions produced bipyramidal crystals very similar to that of the wild-type toxin. Figure 1 shows the solubilized protoxin in extraction buffer produced by *B. thuringiensis* transformant clones.

Toxicity. Conservative replacement of Trp residues by Phe produced proteins with toxicity comparable to that of the wild-type toxin against *M. sexta* larvae (Table 2), with the exception of mutants W65F and W316F, which showed reduced insecticidal activity and 5- and 15-fold higher LC_{50}s, respectively. Similarly, some nonconservative changes (W73C, W182C, and W210C) of Trp residues by Cys produced toxins with comparable toxicity to that of the wild-type protein. However, other cysteine mutants had reduced insecticidal activity. The mutants W455C and W219C were slightly affected (7-fold higher LC_{50}), and the mutant W316C showed a 36-fold higher LC_{50} when tested against *M. sexta* larvae (Table 2).

Functional studies with Trp mutants affected in the insecticidal activity. To determine the role of Trp residues in the mode of action of Cry1Ab toxin, we selected the mutants that showed compromised insecticidal activity (W65F, W316F, W219C, W316C and W455C) to perform further studies. We

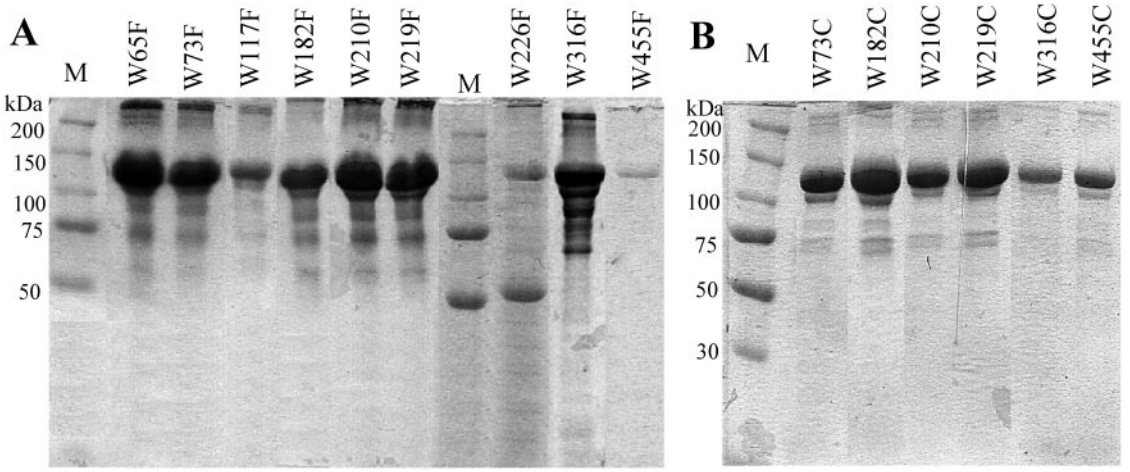

FIG. 1. SDS-PAGE electrophoretic pattern of solubilized Cry1Ab protoxin produced by *Bacillus thuringiensis* wild-type and tryptophan mutant strains. A, W-to-F mutants; B, W-to-C mutants. M, molecular mass standards.

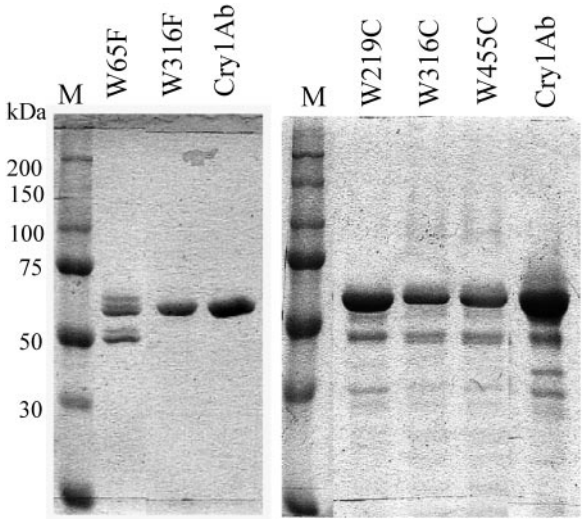

FIG. 2. SDS-PAGE electrophoretic pattern of trypsin-activated Cry1Ab toxin produced by *Bacillus thuringiensis* wild-type and tryptophan mutant strains. Crystal inclusions were purified by sucrose gradients and solubilized in extraction buffer as described in Materials and Methods. The protoxin was activated with trypsin in a mass ratio of 1:20 for 1 h at 37°C. PMSF was added to a final 1 mM concentration to stop proteolysis. M, molecular mass standards.

analyzed trypsin digestion susceptibility, binding to BBMV, oligomer formation and pore formation activity. All these substitutions produced stable toxin fragments when digested with trypsin, indicating no major structural changes in these proteins (Fig. 2). However, the trypsin digestion of mutant W65F, where a slightly higher-molecular-size band was observed (Fig. 2), occurred more slowly than that for the rest of the proteins. Digestion with midgut juice from *M. sexta* larvae was similar to that of the wild-type toxin.

A qualitative binding assay of biotinylated Cry1Ab mutant proteins to *M. sexta* BBMV was performed to analyze the effects of Trp mutations on receptor interaction. Figure 3A shows that mutants W219C, W316F, and W455C bound poorly to *M. sexta* BBMV, unlike the W65F and W316C mutants, which bound to BBMV similarly to the wild-type toxin. In order to provide quantitative data on the effects of Trp mutations on receptor binding, heterologous binding competition of Cry1Ab wild-type toxin to BBMV was performed. Figure 3B shows that only mutant W65F efficiently competed for the binding of Cry1Ab to BBMV. In contrast, mutants W219C and W316C required higher concentrations to compete for the binding of labeled Cry1Ab, and mutants W455C and W316F did not compete for binding of labeled Cry1Ab toxin even at a 1,000-fold excess, suggesting that all these mutants bind BBMV with lower binding affinity than Cry1Ab toxin.

The formation of the Cry1Ab oligomeric structure and the pore formation activity were also analyzed. Previous work demonstrated that oligomeric Cry1Ab is formed when protoxin is activated by midgut juice proteases in the presence of cadherin receptor (BT-R_1) fragments (8). The oligomeric structure is also formed when activation is done in the presence of a single chain antibody (scFv73) that mimics the BT-R_1 receptor (8). The Cry1Ab mutants were proteolytically activated in the presence of scFv73 antibody, and the oligomeric and monomeric forms of the toxin were visualized by Western blot analysis (Fig. 4). Only mutant W65F produced an amount of oligomeric structure similar to that of the wild-type toxin; in contrast, the formation of the oligomeric structure by the rest of the mutants was severely reduced. Additionally, the structure of oligomeric structure of mutant W316F seems to be altered, since an extra band with a higher molecular size is produced, suggesting a different organization in the oligomeric structure of this mutant or the aggregation of proteins.

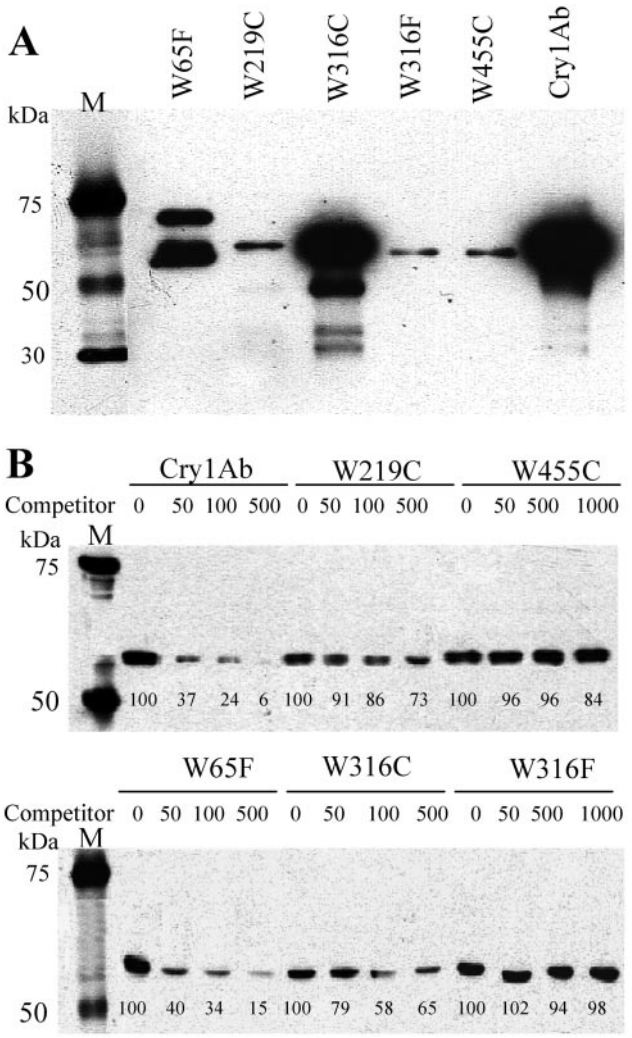

FIG. 3. Binding analysis of some tryptophan mutants of Cry1Ab. A, qualitative binding assay of biotinylated Cry1Ab mutant proteins to *M. sexta* BBMV. B, Heterologous competition assays of biotinylated Cry1Ab toxin to BBMV with the unlabeled mutant proteins (1- to 1,000-fold excess of competitor). M, molecular mass standards. Numbers below bands represent percentages of signal relative to Cry1Ab binding without competitor.

The pore formation activity was assayed using the oligomeric structures of the different Trp mutants. The effect of 3 nM each Trp substitution in inducing K^+ permeability of *M. sexta* BBMV was analyzed by determining the distribution of a fluorescent dye, Dis-C_3-(5), that is sensitive to changes in membrane potential. This concentration of wild-type Cry1Ab oligomeric structure produced a fast hyperpolarization (Fig. 5) when added to *M. sexta* BBMV and also increased the response

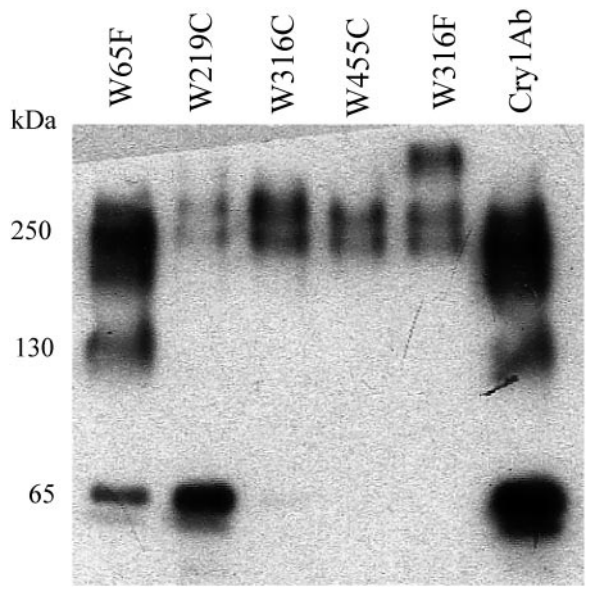

FIG. 4. Western blot of Cry1Ab toxin and tryptophan mutant proteins after proteolytic activation with *Manduca sexta* midgut juice in the presence of scFv73 antibody.

to KCl additions ($m = 0.076$) relative to the control, to which the same amount of buffer was added ($m = -0.001$) (Fig. 5A). The observed hyperpolarization can be explained by the exit of potassium ions from inside the BBMV through the new Cry toxin open permeability. Figure 5 shows that the addition of 3 nM oligomeric Cry1Ab mutant W65F, W219C, W316C, or W455C to the BBMV induces K^+ permeability very similar to that induced by the wild-type toxin. Only the mutation W316F showed a 36% reduction in the induced K^+ permeability relative to Cry1Ab (Fig. 5B).

DISCUSSION

During intoxication, the Cry protoxins must change from insoluble crystals into membrane-inserted toxins which form ionic pores. To date, the structural changes of Cry toxins during oligomerization and insertion into the membrane remain unknown.

Trp residues play an important role in proteins. This is one of the biggest amino acid residues codified by a single codon. In most protein families, the Trp residues are located at highly conserved positions. The Cry1Ab toxin has nine Trp residues, seven of which are located in domain I, the pore-forming domain, and two of which are located in domain II, which is involved in receptor recognition (9). Eight Trp residues of Cry1Ab are highly conserved among the members of the three-

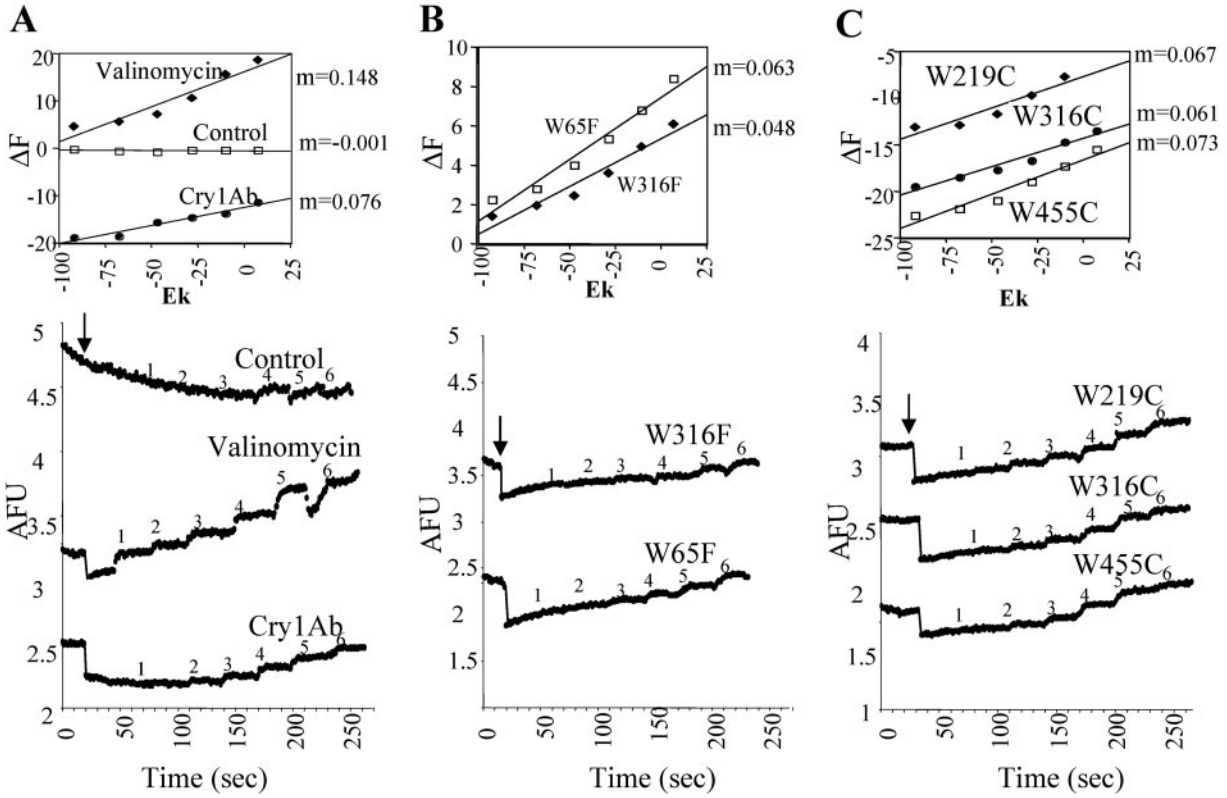

FIG. 5. Analysis of K^+ permeability induced by Cry1Ab oligomeric structure. Numbers (1 to 6) above the traces correspond to each one of the KCl additions. Changes in membrane potential were induced by 3 nM pure Cry1Ab or mutant oligomeric structures monitored by successive additions of KCl (final concentrations, 1, 4 mM; 2, 8 mM; 3, 12 mM; 4, 16 mM; 5, 32 mM; and 6, 64 mM) to *M. sexta* BBMV. AFU, arbitrary fluorescence units. Arrows indicate the time of toxin, buffer, or valinomycin addition. Membrane potential determinations were done four times. Insets show the plots of changes in fluorescence (ΔF) (%) versus K^+ equilibrium potential (E_K) (millivolts). A, Cry1Ab wild-type, valinomycin, and the control traces done without toxin addition. B, W316F and W65F. C, W219C, W316C, and W455C.

domain Cry family, suggesting an important role for these residues in toxin activity. The only Trp of Cry1Ab that is not highly conserved in the rest of the Cry family members is W219; this residue is present in only Cry1A toxins (4).

Trp residues may play an important role in the process of transforming water-soluble toxins into membrane-bound pores. Other pore-forming bacterial toxins, such as aerolysin, perfringolysin O, and alpha-toxin, form oligomeric structures in their target membranes (22). These toxins have Trp-rich domains involved in membrane insertion; characteristically, the Trp in these proteins is located at the membrane-water interface (22). Quenching analysis of Trp fluorescence of Cry1Ab toxin which was inserted into the membrane indicated that, in this protein, most of its Trp residues are also located in the membrane-water interface (23).

In this work, we analyzed the roles of individual Trp residues in the mode of action of Cry1Ab toxin by carrying out conservative and nonconservative mutations of all Trp residues that are present in this toxin. All Trp-Phe changes resulted in the formation of bipyramidal crystals. In contrast, the nonconservative mutants, W65C, W117C, and W226C, did not produce crystal inclusion bodies, suggesting that the presence of an aromatic or hydrophobic residue in these positions may play an important role in the overall structure of the protein. It is also possible that incorporation of a new Cys residue led to incorrect disulfides, which prevented crystal formation. The crystals produced by mutants W316C and W455C were very small, suggesting that these changes also affected, in some way, the stability of these proteins. There are few references for Trp substitutions in Cry toxins in the literature. It was reported that the change of W226 for Ala in Cry1Ab toxin prevented detectable protoxin deposition (1), while W210C mutation in Cry1Ac did not affect protoxin production or toxicity (2).

Regarding the insecticidal activity of the Trp substitutions, we found that some conservative changes (W73F, W117F, W182F, W210F, W219F, W226F, and W455F) of Trp residues by Phe and some nonconservative changes (W73C, W182C, and W210C) showed toxicity comparable to that of the wild-type toxin against *M. sexta* larvae (Table 2). In contrast, the presence of tryptophan residues at positions 65 and 316 seems to play a significant role, since conservative changes by Phe resulted in protein expression with compromised insecticidal activity. These Trp residues are buried in the hydrophobic core of domains I and II, respectively, suggesting that they may be important for maintaining the hydrophobic interactions within the toxin and the correct structure of the protein.

Substitutions of W219 and W455 by Cys residues suggested that a hydrophobic side chain is required at these locations since insecticidal activity was affected by the nonconservative Cys change but unaffected by the Phe change. Residue W455 is also buried within domain II, suggesting that it could also be involved in important hydrophobic interactions within the toxin. Residue W219 is particularly interesting since it is located in the loop connecting helices α-6 and α-7 of domain I and is found highly exposed to the solvent in the three-dimensional structure of monomeric Cry1Aa toxin (Fig. 6). This location corresponds to the same toxin side of residues A92, F148, and Y153 that were previously implicated in membrane insertion (6, 10, 19). It has been proposed that this side of the toxin will face the cell membrane and could directly participate in the domain I membrane insertion. The facts that the Cry1Ab toxin requires an aromatic or a hydrophobic residue at position 219 for insecticidal activity and that this residue is highly exposed suggest the possibility that this amino acid might be important for membrane contact and insertion or as a determinant of protein orientation. However, our data show that mutant W219C is affected in the binding to BBMV since higher concentrations of mutant protein were needed to compete with the binding of the wild-type toxin to BBMV, suggesting that this residue could play a role in the contact with the receptors. This mutant produced a smaller amount of the oligomeric structure, which can be explained by the lower binding capabilities since interaction with the receptor is important for oligomer formation (8). Figure 6 shows that, within the structure of Cry1Aa toxin, the W219 residue is very close to loop alpha-8 (3 to 4 Å from Gln285 and Glu288). Loop alpha-8 has an important role in the interaction with the cadherin receptor (7). At this stage, we cannot form a clear conclusion on whether W219 is directly involved in the contact with the receptor or whether the change to Cys affects loop alpha-8 structural conformation, resulting in reduced receptor binding.

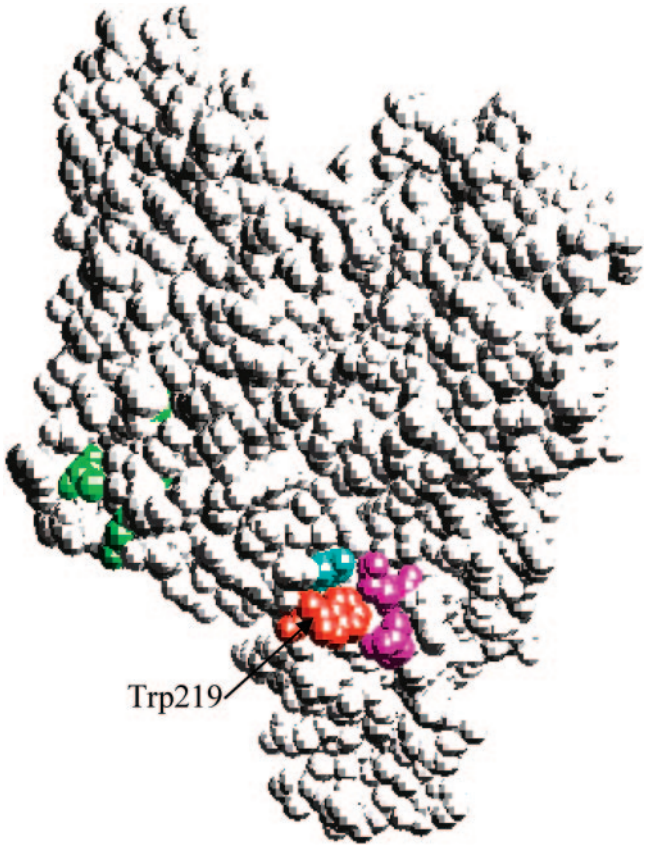

FIG. 6. Locations of specific amino acid residues in the space-filled three-dimensional structural model of Cry1Aa. Ala92, Leu148, and Tyr153 are green; Trp219 is red; Tyr229 is light blue; Gln285 and Glu288 are purple. This figure was made with the Swiss-PdbViewer program.

Mutants W316F, W316C, and W455C were also less efficient to compete for the binding of labeled Cry1Ab toxin, suggesting that these mutants are also affected in binding to receptors. These two residues are buried within domain II, which is considered an important binding domain of Cry toxins. Therefore, it is possible

that the Trp residues located in the interior of domain II have an important role in maintaining the structure of this domain for efficient receptor interaction and oligomer formation.

It is important to mention that all mutants affected in binding to BBMV produce lesser amounts of oligomeric structure than that of the wild-type Cry1Ab (Fig. 4). However, these oligomeric structures retain capacities to induce pore formation similar to that of the wild-type toxin. The mutation W316F showed a slightly reduced pore formation that could be correlated with an altered oligomer formation (Fig. 4 and 5).

One major problem of field applications of Cry toxins is that their exposure to sunlight (20) can bring about reduced bioactivity. It has been demonstrated that chromophores are the prime light-absorbing agents. In the UV excited state, they interact with molecular oxygen, creating singlet oxygen. These free radicals are highly reactive and attack the most vulnerable structure in the protein, the indole ring of the Trp residue. Raman spectroscopy studies demonstrated the breakdown of Trp side chains after sunlight irradiation (20, 21). We hypothesize that strategic replacement of some Trp could reduce the high sensitivity of Cry toxins to near-UV damage without affecting toxicity. UV protection of Cry1Ac toxin by melanin has been previously reported (25). Preliminary results obtained after analyzing the effect on insecticidal activity of sunlight exposure of the Trp mutants indicated that only mutants W73F and W73C were more resistant to UV damage than the Cry1Ab wild-type protein or the rest of the Trp mutants tested (data not shown). These experiments were performed with crystal suspensions irradiated 65 h with an Oriel solar simulator (Oriel Corporation, Stamford, CT), These data could suggest that W73 might be in an accessible position and may have a significant role in the bioactivity because once it changed, the photosensitivity ceased. Therefore, Cry1Ab W73F could be a good candidate for producing *B. thuringiensis* formulations with higher efficiency under field conditions. This remains to be determined, and other mutations in this residue are in progress in order to confirm this result and select the most stable protein after UV irradiation.

ACKNOWLEDGMENTS

We thank Lizbeth Cabrera and Oswaldo López for technical assistance.
This research was supported in part by DGAPA/UNAM IN207503-3 and IN206503-3, CONACyT 36505-N, and USDA 2002-35302-12539.

REFERENCES

1. **Alcantara, E. P., O. Alzate, M. K. Lee, A. Curtiss, and D. H. Dean.** 2001. Role of α-helix seven of *Bacillus thuringiensis* Cry1Ab δ-endotoxin in membrane insertion, structural stability and ion channel activity. Biochemistry **40:**2540–2547.
2. **Aronsosn, A. I., D. Wu, and Ch. Zhang.** 1995. Mutagenesis of specificity and toxicity regions of *Bacillus thuringiensis* protoxin gene. J. Bacteriol. **177:**4059–4065.
3. **Bravo, A., J. Sánchez, T. Kouskoura, and N. Crickmore.** 2002. N-terminal activation is an essential early step in the mechanism of action of the *B. thuringiensis* Cry1Ac insecticidal toxin. J. Biol. Chem. **277:**23985–23987.
4. **Bravo, A.** 1997. Phylogenetic relationships of the *Bacillus thuringiensis* δ-endotoxin family proteins and their functional domains. J. Bacteriol. **179:**2793–2801.
5. **Bravo, A., I. Gómez, J. Conde, C. Muñoz-Garay, J. Sánchez, R. Miranda, M. Zhuang, S. S. Gill, and M. Soberón.** 2004. Oligomerization triggers binding of a *Bacillus thuringiensis* Cry1Ab pore-forming toxin to aminopeptidase N receptor leading to insertion into membrane microdomains. Biochim. Biophys. Acta **1667:**38–46.
6. **Chen, X. J., A. Curtiss, E. Alcantara, and D. H. Dean.** 1995 Mutations in domain I of *Bacillus thuringiensis* δ-endotoxin Cry1Ab reduced the irreversible binding of toxin to *Manduca sexta* brush border membrane vesicles. J. Biol. Chem. **270:**6412–6419.
7. **Gómez, I., D. H. Dean, A. Bravo, and M. Soberon.** 2003. Molecular basis for *Bacillus thuringiensis* Cry1Ab toxin specificity: Two structural determinants in the *Manduca sexta B. thuringiensis*-R1 receptor interact with loops α-8 and 2 in domain II of Cy1Ab toxin. Biochemistry **42:**10482–10489.
8. **Gómez, I., J. Sánchez, R. Miranda, A. Bravo, and M. Soberón.** 2002. Cadherin-like receptor binding facilitates proteolytic cleavage of helix α-1 in domain I and oligomer pre-pore formation of *Bacillus thuringiensis* Cry1Ab toxin. FEBS Lett. **513:**242–246.
9. **Grochulski, P., L. Masson, S. Borisova, M. Pusztai-Carey, J. L. Schwartz, R. Brousseau, and M. Cygler.** 1995. *Bacillus thuringiensis* Cry1A(a) insecticidal toxin: Crystal structure and channel formation. J. Mol. Biol. **254:**447–464.
10. **Hussain, S.-R. A., A. I. Aronson, and D. H. Dean.** 1996. Substitution of residues on the proximal side of Cry1A *Bacillus thuringiensis* δ-endotoxins affects irreversible binding to *Manduca sexta* midgut membrane. Biochem. Biophys. Res. Commun. **226:**8–14.
11. **Knight, P., N. Crickmore, and D. J. Ellar.** 1994. The receptor for *Bacillus thuringiensis* CryIA(c) δ-endotoxin in the brush border membrane of the lepidopteran *Manduca sexta* is aminopeptidase *N.* Mol. Microbiol. **11:**429–436.
12. **Lereclus, D., H. Agaisse, M. Gominet, and J. Chaufaux.** 1995. Overproduction of encapsulated insecticidal crystal proteins in a *Bacillus thuringiensis spo*OA mutant, Bio/Technology **13:**67–71.
13. **Lereclus, D., O. Arantes, J. Chaufaux, and M.-M. Lecadet.** 1989. Transformation and expression of a cloned δ-endotoxin gene in *Bacillus thuringiensis*. FEMS Microbiol. Lett. **60:**211–218.
14. **Li, J., J. Carroll, and D. J. Ellar.** 1991. Crystal structure of insecticidal δ-endotoxin from *Bacillus thuringiensis* at 2.5 Å resolution. Nature **353:**815–821.
15. **Lorence, A., A. Darszon, C. Díaz, A. Liévano, A., R. Quintero, and A. Bravo.** 1995. δ-Endotoxins induce cation channels in *Spodoptera frugiperda* brush border membranes in suspension and in planar lipid bilayers. FEBS Lett. **360:**217–222.
16. **Meza, R., M.-E. Nuñez-Valdez, J. Sánchez, and A. Bravo.** 1996. Isolation of Cry1Ab protein mutants of *Bacillus thuringiensis* by a highly efficient PCR site-directed mutagenesis system. FEMS Microbiol. Lett. **145:**333–339.
17. **Morse, R. J., T. Yamamoto, and R. M. Stroud.** 2001. Structure of Cry2Aa suggests an unexpected receptor binding epitope. Structure **9:**409–417.
18. **Nagamatsu, Y., T. Koike, K. Sasaki, A. Yoshimoto, and Y. Furukawa.** 1999. The cadherin-like protein is essential to specificity determination and cytotoxic action of the *Bacillus thuringiensis* insecticidal CryIAa toxin. FEBS Lett. **460:**385–390.
19. **Nuñez-Valdez, M.-E., J. Sánchez, L. Lina, A. Lorence, L. Güereca, and A. Bravo.** 2001. Structural and functional studies of α-helix 5 region from *Bacillus thuringiensis* Cry1Ab δ-endotoxin. Biochim. Biophys. Acta **1546:**122–131.
20. **Pozsgay, M., P. Fast, H. Kaplan, and P. R. Carey.** 1987. The effect of sunlight on the protein crystals from *Bacillus thuringiensis* var. *kurstaki* HD1 and NRD12: a Raman spectroscopic study. J. Invertebr. Pathol. **50:**246–253.
21. **Puzstai, M., P. Fast, L. Gringorten, H. Kaplan, T. Lessard, and P. R. Carey.** 1991. The mechanism of sunlight-mediated inactivation of *Bacillus thuringiensis* crystals. Biochem. J. **273:**43–47.
22. **Raja, S. M., S. S. Rawat, A. Chattopadhyay, and A. K. Lala.** 1999. Localization and environment of tryptophans in soluble and membrane-bound states of a pore-forming toxin from *Staphylococcus aureus*. Biophys. J. **76:**1469–1479.
23. **Rausell, C., C. Muñoz-Garay, R. Miranda-CassoLuengo, I. Gómez, E. Rudiño-Piñera, M. Soberón, and A. Bravo.** 2004. Tryptophan spectroscopy studies and black lipid bilayer analysis indicate that the oligomeric structure of Cry1Ab toxin from *Bacillus thuringiensis* is the membrane-insertion intermediate. Biochemistry **43:**166–174.
24. **Sangadala, S., F. W. Walters, L. H. English, and M. J. Adang.** 1994. A mixture of *Manduca sexta* aminopeptidase and phosphatase enhances *Bacillus thuringiensis* insecticidal CryIA(c) toxin binding and $^{86}Rb^{+}$-K^{+} efflux in vitro. J. Biol. Chem. **269:**10088–10092.
25. **Saxena, D., E. Ben-Dov, R. Manasherob, Z. Barak, S. Boussiba, and A. Zarisky.** 2002. A UV tolerant mutant of *Bacillus thuringiensis* subsp. *kurstaki* producing melanin. Curr. Microbiol. **44:**25–30.
26. **Schnepf, E., N. Crickmore, J. Van Rie, D. Lereclus, J. Baum, J. Feitelson, D. R. Zeigler, and D. H. Dean.** 1998. *Bacillus thuringiensis* and its pesticidal crystal proteins. Microbiol. Mol. Biol. Rev. **62:**775–806.
27. **Thomas, W. E., and D. J. Ellar.** 1983. *Bacillus thuringiensis var israelensis* crystal δ-endotoxin: effects on insect and mammalian cells *in vitro* and *in vivo*. J. Cell Sci. **60:**181–197.
28. **Vadlamudi, R. K., E. Weber, I. Ji, T. H. Ji, and L. A. Bulla.** 1995. Cloning and expression of a receptor for an insecticidal toxin of *Bacillus thuringiensis*. J. Biol. Chem. **270:**5490–5494.
29. **Vie, V., N. Van Mau, P. Pomarde, C. Dance, J. L. Schwartz, R. Laprade, R. Frutos, C. Rang, L. Masson, F. Heitz, and C. Le Grimellec.** 2001. Lipid-induced pore formation of the *Bacillus thuringiensis* Cry1Aa insecticidal toxin. J. Membr. Biol. **180:**195–203.
30. **Wolfersberger, M., P. Lüthy, A. Maurer, F. Parenti, V. Sacchi, B. Giordana, and G. M. Hanozet.** 1987. Preparation and partial characterization of amino acid transporting brush border membrane vesicles from the larval midgut of the cabbage butterfly (*Pieris brassicae*). Comp. Biochem. Physiol. **86A:**301–308.